STRUCTURAL, ELECTRONIC, AND MAGNETIC PROPERTIES OF SR$_{1-x}$MN$_x$F$_2$ ALLOYS STUDIED BY FIRST-PRINCIPLES CALCULATIONS

D. M. HOAT[1,2†], J. GUERRERO-SANCHEZ[3], R. PONCE-PÉREZ[3], J. F. RIVAS-SILVA[4] AND GREGORIO H. COCOLETZI[4]

[1]*Computational Laboratory for Advanced Materials and Structures, Advanced Institute of Materials Science, Ton Duc Thang University, Ho Chi Minh City, Vietnam*

[2]*Faculty of Applied Sciences, Ton Duc Thang University, Ho Chi Minh City, Vietnam*

[3]*Universidad Nacional Autónoma de México, Centro de Nanociencias y Nanotecnología, Apartado Postal 14, Ensenada, Baja California, Código Postal 22800, Mexico*

[4]*Benemérita Universidad Autónoma de Puebla, Instituto de Física, Apartado Postal J-48, Puebla 72570, Mexico*

E-mail: †dominhhoat@tdtu.edu.vn

Abstract. *In this work, the structural, electronic, and magnetic properties of the $Sr_{1-x}Mn_xF_2$ (x = 0, 0.25, 0.5, 0.75, and 1) compounds are investigated using first-principles calculations. Crystallizing in fluorite structure, SrF_2 is a magnetism-free indirect gap insulator with band gap of 11.61 eV as determined by the reliable mBJK functional. Mn substitution induces the magnetic insulator behavior as both spin configurations exhibit large band gaps with a strong spin-polarization. Specifically, spin-up energy gaps of 8.554, 7.605, 6.902, and 6.154 eV are obtained for $Sr_{0.75}Mn_{0.25}F_2$, $Sr_{0.5}Mn_{0.5}F_2$, $Sr_{0.25}Mn_{0.75}F_2$, and MnF_2, respectively. Whereas, the spin-down state shows larger values of 8.569, 8.864, 9.307, and 9.837 eV, respectively. Consequently, significant magnetization is induced and an integer total spin magnetic moment of 5 μ_B is obtained, being produced mainly by the spin-up Mn-3d state. Finally, the formation enthalpy and cohesive energy are determined, which indicate good thermodynamic and structural stability of the studied materials. Results suggest that Mn substitution at the Sr-sites of SrF_2 compound may be an efficient approach to create new magnetic materials to be used in the spintronic devices.*

Keywords: First-principles calculations; SrF$_2$; Diluted magnetic insulator; Spintronics.

Classification numbers: 31.15.-p; 75.60.Ch.

I. INTRODUCTION

The fast science and technology development has demanded high level of information processing and storage. In this regard, the spin-based electronics or spintronics has emerged as a promising alternative for the conventional electronics based only on the electron charge. Considering the electron spin as an additional degree of freedom may lead to the emergence of novel properties [1, 2]. In spintronic devices, the creation of spin current plays a key role, which can be realized by either spin injection from the highly spin-polarized materials or spin filtering. Therefore, the employed materials are required to possess suitable electronic and magnetic properties. So far, most of spintronic devices are fabricated by hybrid structures combining semiconductor and magnetic materials, presenting a difficulty to control the spin flux. Therefore, researchers have focused investigations on developing novel ferromagnetic materials suitable for spintronic applications [3]. In general, these materials exhibit large spin polarization generated by the unusual electronic features as half-metallicity [4, 5] and magnetic semiconductor [6, 7], which allow an easy management of electron spin and retaining benefits of the traditional microelectronics.

Within the studied spintronic materials, it would be flawed not mentioning the diluted magnetic semiconductors (DMS) family. This family is formed by doping semiconductors with magnetic atoms as transition metals with unpaired $3d$ orbital. Experimentally, with the development of sophisticated synthesis equipment, different DMSs have been successfully synthesized as CdS:Co [8, 9], Cd:Cr [10], Cd:Mn [11], ZnS:Nd [12], ZnS:Fe [13], among others. In parallel, because of the low cost and safety, theoretical calculations have been widely employed to predict new DMSs. For examples, Bourouris et al. [14] have investigated structural, electronic, and magnetic properties of the $Cd_{1-x}Fe_xS$ (x = 0.25, 0.5, and 0.75) DMSs using FP-LMTO calculations. Results indicate a half-metallic ferromagnetic character of these alloys, with an atomic magnetic moment as large as 4 μ_B for Fe atom. MgS in rock-salt and zinc-blende structures doped with Vanadium $Mg_{1-x}V_xS$ (x = 0, 0.25, 0.5, and 0.75) have been investigated by Abdellit et al. [15]. Calculations indicate the magnetic semiconductor and half-metallic nature of the doped rock-salt and zinc-blende systems, respectively. A total magnetic moment of 3 μ_B is obtained, being produced mainly by the V atoms. Similarly, large variety of DMS materials have been considered, including $Ba_{1-x}Cr_xTe$ [16], $Ba_{1-x}V_xS$ [17], $Al_{0.75}Mn_{0.25}Y$ (Y = N, P, As) [18], and $Ca_{1-x}Cr_xS$ [19], among others. Revising the literature, we realized that in most cases only semiconductors are employed as host for doping, while insulators with large band gap have not been considered yet.

On the other hand, Strontium fluoride (SrF_2) has been extensively studied due to its high technological potential. Experimentally, SrF_2 has been successfully prepared by different methods as solvothermal synthesis [20, 21] and hydrothermal synthesis [22]. Characterizations have demonstrated the insulator nature of this binary with an energy gap as large as 11.25 eV [23]. Because of its optical transparency and low energy phonon (336 cm^{-1} [24]), SrF_2 has been usually used as host material for the optically active centers (OAC) [25–27]. However, the possibility of applying SrF_2 in spintronics has not been treated well, so far. In this work, we comprehensively investigate the structural, electronic, and magnetic properties of the $Sr_{1-x}Mn_xF_2$ (x = 0, 0.25, 0.5, 0.75, and 1) alloys using first-principles calculations. The lattice parameter variation is analyzed to study alloying effects on the structural geometry. Our simulations show good stability of MnF_2 crystallizing in fluorite structure. Spin-resolved electronic band structure is calculated and analyzed to investigate the spin polarization induced by Mn atoms, while the density of states

allows analyzing the band structure formation. Strong spin polarization suggests magnetization in the studied materials, which will be characterized by significant spin magnetic moments and spin charge distribution. It is anticipated that results recommend new ferromagnetic materials prospective for spintronic applications, with large spin-down spin flip gap between 1.157 to 3.522 eV.

II. COMPUTATIONAL DETAILS

Spin-polarized first-principles calculations based on the density functional theory (DFT) [28] have been carried out to study the structural, electronic, and magnetic properties of $Sr_{1-x}Mn_xF_2$ compounds. The expansion of wave functions is realized in the framework of the full-potential linearized augmented plane-wave (FP-LAPW) method as embedded in WIEN2k simulation package [29]. Cut-off energy for the wave planes in the interstices is set to $R_{MT}K_{max} = 7$, and maximum quantum number of $l_{max} = 7$ is chosen for spherical harmonics within muffin-tin. The revised Perdew–Burke–Ernzerhof generalized gradient approximation (GGA-PBESol) [30] is adopted to describe the exchange-correlation potential. In addition, the Kohn-improved mBJ potential (mBJK) allows reaching reliable electronic and magnetic results provided that it can yield accurate energy gap and treat well the systems containing transition metals [31–34]. Monkhorst-Pack k-grid [35] size of $10 \times 10 \times 10$ is generated in all calculations to integrate the Brillouin zone. Self-consistency criterion of 0.0001 Ry is set for the iterative calculations.

III. RESULTS AND DISCUSSION

III.1. Structural properties

SrF_2 crystallizes in cubic fluorite structure, ascribed to the $Fm\bar{3}m$ space group (no. 225). In an unit cell, there are four unit formula composed of four Sr atoms and eight F atoms (See. Fig.1a). As a first necessary step of theoretical calculations, the geometry is optimized by fitting different calculated Energy-Volume (E-V) data to the Birch-Murnaghan equation of state as follows [36]:

$$E(V) = E_0 + \frac{9V_0B}{16}\left\{\left[\left(\frac{V_0}{V}\right)^{2/3} - 1\right]^3 B' + \left[\left(\frac{V_0}{V}\right)^{2/3} - 1\right]^2\left[6 - 4\left(\frac{V_0}{V}\right)^{2/3}\right]\right\} \quad (1)$$

Minimizing the energy with respect to volume will yield the equilibrium structural parameters. Our calculations yield a lattice constant of 5.78 Å, which presents a small deviation of -0.34% from experimental value (5.80 Å) [37] and is in agreement with previous calculations, suggesting the reliability of the results.

Figures 1b-e display the crystal structure of $Sr_{1-x}Mn_xF_2$ compounds with x = 0.25, 0.5, 0.75, and 1, which are formed by substituting one, two, three and four Sr atoms in the unit cell by Mn atoms, respectively. Using the procedure described above, the lattice parameters of 5.64, 5.50, 5.34, and 5.16 Å are obtained, respectively. Note that this parameter decreases according to increase the Mn concentration, which is a result of the smaller atomic size of Mn atom as compared to Sr atom. In general, the Vegard's law is employed to describe the composition-dependent variation of alloy lattice constant, which makes use of a linear equation as follows [38]:

$$a(A_xB_{1-x}C) = (1-x)a_{BC} + xa_{AC} \quad (2)$$

However, this law has been proven to not characterize accurately the dependence both experimentally and theoretically [39,40]. Therefore, a quadratic equation with an additional parameter called
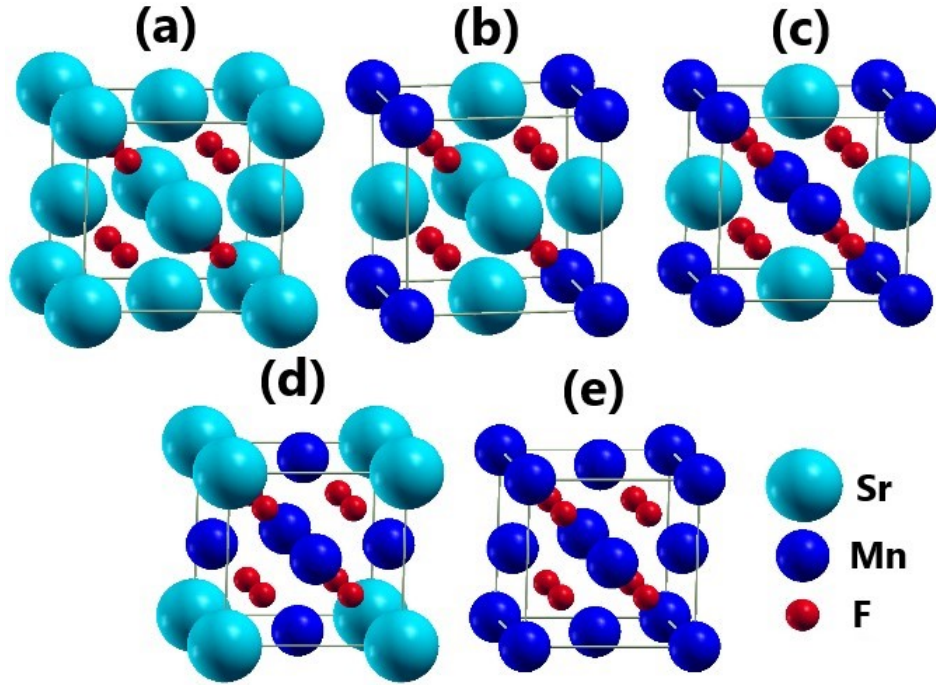
Fig. 1. Crystal structure of $Sr_{1-x}Mn_xF_2$ compounds with (a) x = 0; (b) x = 0.25; (c) x = 0.5; (d) x = 0.75; and (e) x = 1.

"bowing parameter" b has been widely used, which is written as follows [41]:

$$a(A_xB_{1-x}C) = (1-x)a_{BC} + xa_{AC} - x(1-x)b \tag{3}$$

Fitting the obtained results to equations(2-3), the change can be represented by:

$$a(x) = 5.78 - 0.62x \tag{4}$$

$$a(x) = 5.78 - 0.50x - 0.11x^2 \tag{5}$$

Figure 2 exhibits the calculated lattice parameters and plots of expression (4-5). It can be noted that a second order equation can describe more accurately the variation. It is worth mentioning that the appearance of bowing parameter is induced by the weak mismatches between SrF_2 and MnF_2 compounds generated by a large atomic size difference of Sr and Mn atoms.

In addition, the bulk modulus values of 74.49, 80.89, 90.00, 102.26, and 120.61 (GaP) are obtained for SrF_2, $Sr_{0.75}Mn_{0.25}F_2$, $Sr_{0.5}Mn_{0.5}F_2$, $Sr_{0.25}Mn_{0.75}F_2$, and MnF_2 compounds, respectively. These results suggest that the hardness/compressibility of SrF_2 is enhanced/reduced by alloying with Mn, satisfying the well known inverse relation volume-hardness. From Fig.2, one can see that a quadratic relation describes the bulk modulus variation better than a linear equation, which can be written as following:

$$B(x) = 74.79 + 14.53x + 30.91x^2 \tag{6}$$
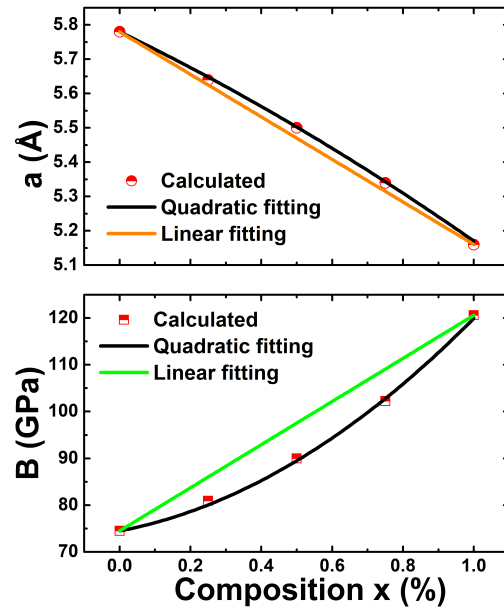
Fig. 2. Variation of lattice parameter a and bulk modulus B of $Sr_{1-x}Mn_xF_2$ compounds as a function of composition x.

III.2. Electronic properties
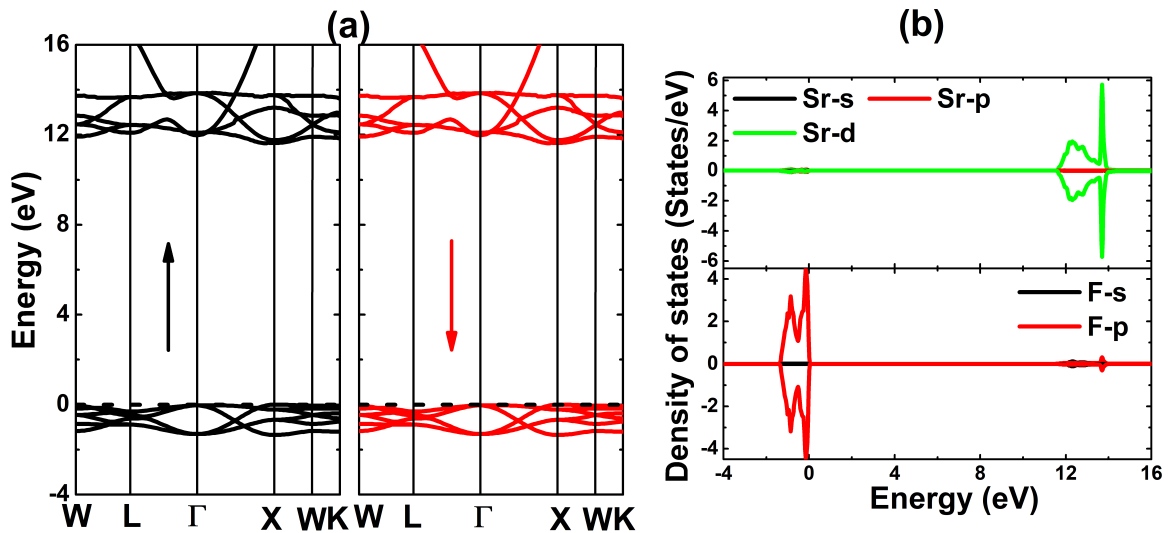
Fig. 3. (a) Spin-resolved electronic band structure (spin-up: black curve; spin-down: red curve); and (b) Partial density of states of SrF_2 compound.

Fig. 3 shows the spin-resolved electronic band structure and partial density of states (PDOS) of the SrF_2 compound. It can be noted a complete spin symmetry, suggesting the non-magnetic

nature. The valence band maximum (VBM) and conduction band minimum (CBM) are located at X point and along ΓX direction, respectively, indicating an indirect gap nature. Specifically, an energy gap value of 11.61 eV is obtained, which exhibits a good agreement with experimental results [23]. Reminding that due to a large electronegativity difference, one can expect that two outermost electrons of Sr atom (Sr-$4d^2$) are transferred to fill out the outermost partially occupied orbital of each F atom (F-$2p^5$). Therefore, in the SrF_2 compound, the Sr^{2+} and F^- ions may be formed with electronic configuration of $[Ar]3d^{10}4s^24p^64d^0$ and $1s^22s^22p^6$, respectively. Now from the PDOS spectra, it can be concluded that the valence band from -1.42 to 0 eV is composed mainly by the totally occupied F-2p state, while the conduction band between 11.61 eV and 15.10 eV shows the major presence of the unoccupied Sr-4d state. The absence of orbital hybridization suggests the ionic character of this material as expected.
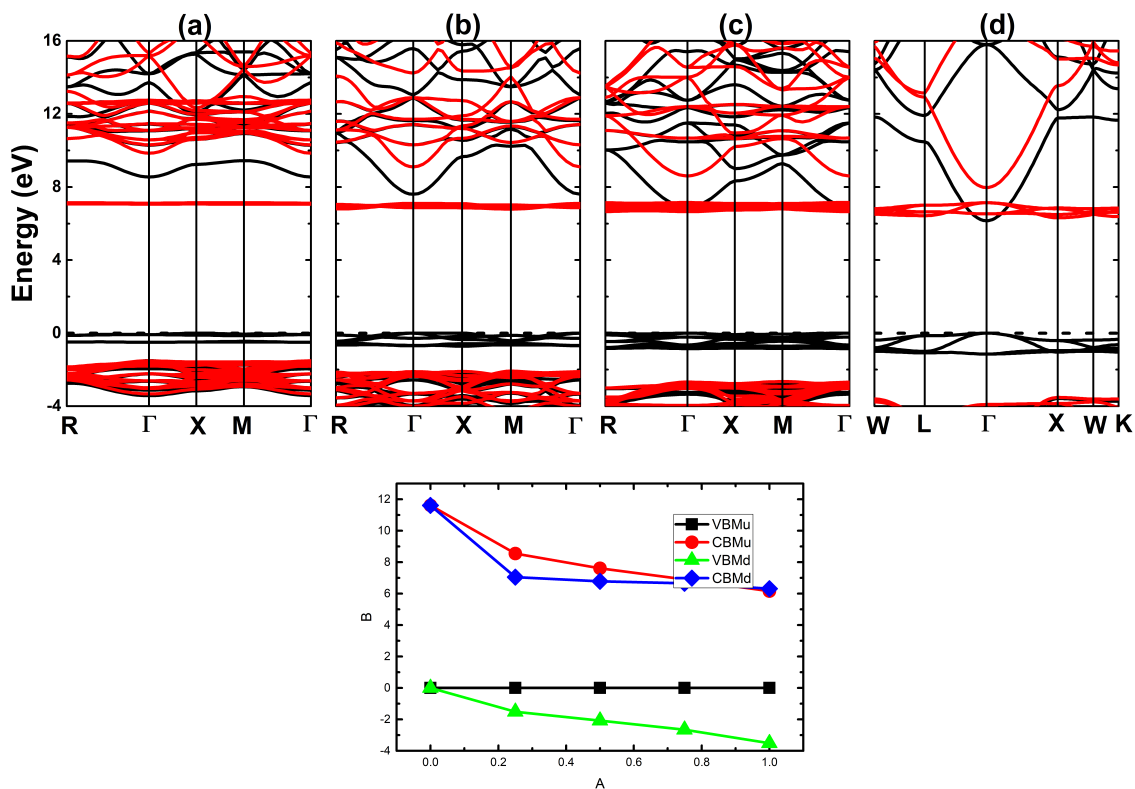
Fig. 4. Electronic band structure of $Sr_{1-x}Mn_xF_2$ compounds with (a) x = 0.25; (b) x = 0.5; (c) x = 0.75; and (d) x = 1 (spin-up: black curve; spin-down: red curve); and (e) band edges as a function of composition x.

The electronic band structures of $Sr_{1-x}Mn_xF_2$ with x = 0.25, 0.5, 0.75, and 1 are given in Fig. 4a-d. Note that the spin symmetry is strongly broken by Mn substitution. Clearly, the spin asymmetry is observed at the vicinity of the Fermi level and conduction band, and the spin splitting increases according to increase the Mn composition. Band structure features indicate that these compounds are magnetic insulator materials provided that both spin channels exhibit insulator
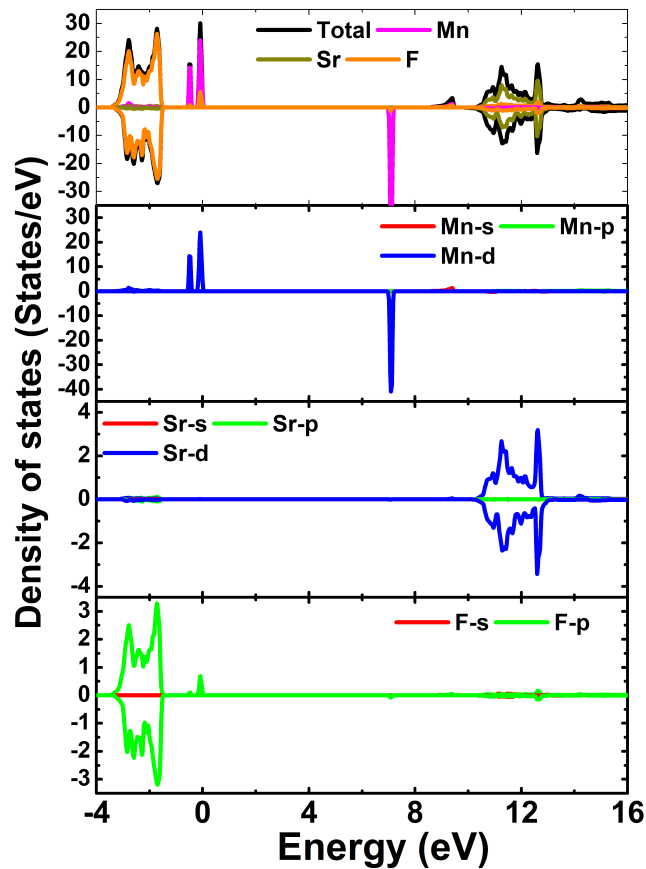
Fig. 5. Spin-resolved density of states of $Sr_{0.75}Mn_{0.25}F_2$ compound.

nature. In Fig. 4e, the band edges positions are plotted as a function of Mn composition. It is important mentioning that in all cases, the Fermi level is set at 0 eV. From the figure, one can see that the spin-up CBM and spin-down CBM move towards the Fermi level, while the spin-down VBM exhibits an opposite behavior as it shifts away from the Fermi level as increasing the Mn concentration. It appears that the variation rate becomes smaller at large Mn composition. Our calculations yield spin-up energy gaps of 8.554, 7.605, 6.902, and 6.154 eV for $Sr_{0.75}Mn_{0.25}F_2$, $Sr_{0.5}Mn_{0.5}F_2$, $Sr_{0.25}Mn_{0.75}F_2$, and MnF_2, respectively. While in the spin-down channel, values of 8.569, 8.864, 9.307, and 9.837 eV are obtained, respectively. As a representative model, the PDOS spectra of $Sr_{0.75}Mn_{0.25}F_2$ compound are illustrated in Fig. 5. Note that similar to SrF_2 compound, the F-2p and Sr-4d states are main contributors to the lower valence band part from -3.48 to -1.44 eV and upper conduction band part from 10.06 to 13.50 eV, respectively. Close to the Fermi level in energy range from -0.61 to 0.00 eV and from 6.69 to 7.23 eV of the spin-up and spin-down channel, respectively, are built mainly by the Mn-3d state, which show a strong spin asymmetry.

Table 1. Total and local magnetic moments of $Sr_{1-x}Mn_xF_2$ compounds with x = 0.25, 0.5, 0.75, and 1).

	M_t (μ_B)	M_I (μ_B)	M_{Sr} (μ_B)	M_{Mn} (μ_B)	M_F (μ_B)
$Sr_{0.75}Mn_{0.25}F_2$	5.00	0.10	0.00	4.84	0.10
$Sr_{0.5}Mn_{0.5}F_2$	5.00	0.12	0.00	4.81	0.02
$Sr_{0.25}Mn_{0.75}F_2$	5.00	0.14	0.00	4.78	0.03
MnF_2	5.00	0.16	-	4.74	0.05
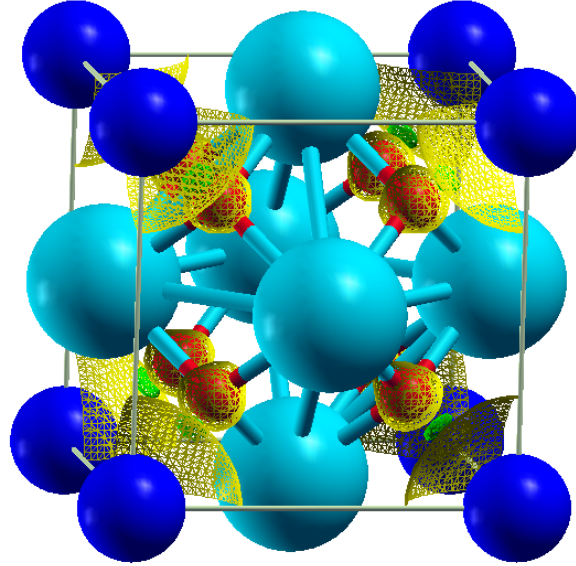
Fig. 6. Spin density in the $Sr_{0.75}Mn_{0.25}F_2$ compound (Yellow surface: spin-up; Green surface: spin-down; Iso-surface value: 0.005 $e/Å^3$; Cyan ball: Sr; Blue ball: Mn; Red ball: F).

III.3. Magnetic properties

Significant magnetization in SrF_2 may be induced by Mn incorporation as suggested by the strong spin asymmetry. Table.1 gives the calculated total, interstitial, and atomic spin magnetic moments in the $Sr_{1-x}Mn_xF_2$ compounds. This parameter is defined by: $M = \rho(\uparrow) - \rho(\downarrow)$, where $\rho(\uparrow)$ and $\rho(\downarrow)$ refer to the charge density in spin-up and spin-down channels, respectively. From the table, one can see that an integer total magnetic moment of 5 μ_B per primitive cell is obtained in all cases, which is produced mainly by the Mn atom with values varying between 4.74 and 4.84 μ_B. Smaller contributions come from the F atom and interstitial electrons. As an example, the spin density distribution in $Sr_{0.75}Mn_{0.25}F_2$ with an iso-surface value of 0.005 $(e/Å^3)$ is illustrated in Fig.6. Iso-surface sizes suggest that the Mn spin-up state is major contributor to the magnetism in accordance to the results listed in Table.1. Re-calling the PDOS spectra, one can attribute the

magnetic properties to the spin splitting of Mn-3d state. The magnetic insulator nature with large spin-down flip gaps and important induced magnetism suggest that incorporating Mn into SrF_2 crystal structure may lead to the formation of new materials suitable for spintronic applications. Specifically, they can be used as spin filter to create the spin current taking advantage of different tunnel barrier heights that the unpolarized electrons encounter and cross with different probability [42, 43].

III.4. Alloys stability

Now, to examine the stability of the alloys at hand, we calculate their formation enthalpy ΔH_f and cohesive energy E_c using the following expressions [44]:

$$\Delta H_f = \frac{E_t - [tE_b(Sr) + uE_b(Mn) + vE_b(F)]}{t + u + v} \tag{7}$$

$$E_c = \frac{E_t - [tE_a(Sr) + uE_a(Mn) + vE_a(F)]}{t + u + v} \tag{8}$$

Herein, E_t is total primitive cell energy; E_b and E_a denote the energy per atom in bulk and energy of an isolated atom; t, u, and v refer to number of Sr, Mn, and F atom in the primitive cell, respectively.

Simulations yield ΔH_f values of -4.88, -4.39, -3.92, -3.50, and -3.14 (eV/atom) for SrF_2, $Sr_{0.75}Mn_{0.25}F_2$, $Sr_{0.5}Mn_{0.5}F_2$, $Sr_{0.25}Mn_{0.75}F_2$, MnF_2, respectively. Negative ΔH_f feature suggests that these compounds are thermodynamically stable, that is, their formation in experiments is feasible provided that the synthesis is an exothermic process. Note that the difficulty degree of formation may increase according to increase the Mn concentration since ΔH_f becomes more positive.

Moreover, E_c values of -5.53, -5.28, -5.04, -4.85, and -4.73 (eV/atom) are obtained when the Mn composition x = 0, 0.25, 0.5, 0.75, and 1, respectively. Negative E_c indicates that the compound state is energetically more favorable than decomposed state, that is, the studied compounds may keep their structure once formed in experiments indicating the structural(chemical) stability. Note that large Mn composition may lead to a less structurally stable alloy, provided that E_c takes less negative value.

Simulations indicate good stability of all the studied binaries and ternaries. Similar to the diluted magnetic semiconductors, the ternary compounds can be synthesized in experiments by doping the SrF_2 in fluorite structure with Mn atoms. Meanwhile, despite MnF_2 has been found to crystallize in the rutile-type structure [45], Zhao et al. [46] has reported the possible formation of this binary compound in fluorite-type structure. Therefore, our results presented herein may be a good theoretical guidance for future theoretical and experimental works treating $Sr_{1-x}Mn_xF_2$ compounds and exploring their spintronic applicability.

IV. CONCLUSIONS

In summary, first-principles calculations have been performed to investigate the Mn substitution effects on the structural, electronic, and magnetic properties of SrF_2 compound. SrF_2 is a non-magnetic ionic material generated by the charge transfer from Sr-5s orbital to F-2p orbital. Its valence band and conduction band are formed mainly by the occupied F-2p state and unoccupied

Sr-4d state, respectively. Incorporating Mn into SrF_2 structure reduces the lattice parameter because of the smaller atomic size of Mn atom compared to Sr atom, for which a quadratic equation describes well the composition-dependent variation. Also, Mn presence enhances the mechanical hardness. Both spin channels of the Mn-substituted systems show insulator nature with a strong spin splitting around the Fermi level generated by Mn-3d state. Consequently important magnetic properties are obtained with the major contribution from spin-up Mn-3d state. Mn substitution may reduce the stability, however all systems at hand possess good thermodynamic and structural stabilities as suggested by their negative formation enthalpies and cohesive energies. Results may recommend new materials with the magnetic insulating for spintronic applications, following the success of diluted magnetic semiconductors.

ACKNOWLEDGMENT

REFERENCES

[1]   A. Hirohata, K. Yamada, Y. Nakatani, I.-L. Prejbeanu, B. Diény, P. Pirro et al., *Review on spintronics: Principles and device applications*, *J. Magn. Magn. Mater.* **509** (2020) 166711.

[2]   S. Bader and S. Parkin, *Spintronics*, *Annu. Rev. Condens. Matter Phys.* **1** (2010) 71.

[3]   J. Cibert, J.-F. Bobo and U. Lüders, *Development of new materials for spintronics*, *C R Phys.* **6** (2005) 977.

[4]   V. Alijani, J. Winterlik, G. H. Fecher, S. S. Naghavi and C. Felser, *Quaternary half-metallic Heusler ferromagnets for spintronics applications*, *Phys. Rev. B* **83** (2011) 184428.

[5]   J. Coey and C. Chien, *Half-metallic ferromagnetic oxides*, *MRS Bull.* **28** (2003) 720.

[6]   J.-W. Yoo, C.-Y. Chen, H. Jang, C. Bark, V. Prigodin, C. Eom et al., *Spin injection/detection using an organic-based magnetic semiconductor*, *Nat. Mater.* **9** (2010) 638.

[7]   T. Fukumura, Y. Yamada, H. Toyosaki, T. Hasegawa, H. Koinuma and M. Kawasaki, *Exploration of oxide-based diluted magnetic semiconductors toward transparent spintronics*, *Appl. Surf. Sci.* **223** (2004) 62.

[8]   F. Ibraheem, M. A. Mahdy, E. A. Mahmoud, J. E. Ortega, C. Rogero, I. A. Mahdy et al., *Tuning paramagnetic effect of Co-doped CdS diluted magnetic semiconductor quantum dots*, *J. Alloys Compd.* **834** (2020) 155196.

[9]   K. A. Bogle, S. Ghosh, S. D. Dhole, V. N. Bhoraskar, L.-f. Fu, M.-f. Chi et al., *Co:CdS diluted magnetic semiconductor nanoparticles: radiation synthesis, dopant- defect complex formation, and unexpected magnetism*, *Chem. Mater.* **20** (2008) 440.

[10] G. Nabi, M. A. Kamran, Z. Usman, A. Majid, T. Alharbi, A. Abdullah et al., *Substitutional site effects of Cr (II) ions on optical and magnetic properties of 1d cds semiconductor nanoneedles for optoelectronic and spintronic applications*, *Inorg. Chem. Commun.* **121** (2020) 108224.

[11] S. Salimian and S. F. Shayesteh, *Structural, optical and magnetic properties of Mn-doped CdS diluted magnetic semiconductor nanoparticles*, *J. Supercond. Nov. Magn.* **25** (2012) 2009.

[12] B. Poornaprakash, S. Ramu, S.-H. Park, R. Vijayalakshmi and B. Reddy, *Room temperature ferromagnetism in Nd doped ZnS diluted magnetic semiconductor nanoparticles*, *Mater. Lett.* **164** (2016) 104.

[13] D. Saikia, R. Raland and J. Borah, *Influence of Fe doping on the structural, optical and magnetic properties of ZnS diluted magnetic semiconductor*, *Physica E Low Dimens. Syst. Nanostruct.* **83** (2016) 56.

[14] C. Bourouis and A. Meddour, *First-principles study of structural, electronic and magnetic properties in $Cd_{1-x}Fe_xS$ diluted magnetic semiconductors*, *J. Magn. Magn. Mater.* **324** (2012) 1040.

[15] Z. Abdelli, A. Meddour, C. Bourouis and M. H. Gous, *Theoretical investigation of the electronic structure and magnetic properties in ferromagnetic rock-salt and zinc blende structures of 3 d (V)-doped MgS*, *J. Electron. Mater.* **48** (2019) 3794.

[16] K. Berriah, B. Doumi, A. Mokaddem, M. Elkeurti, A. Sayede, A. Tadjer et al., *Theoretical investigation of electronic performance, half-metallicity, and magnetic properties of Cr-substituted BaTe*, J. Comput. Electron. **17** (2018) 909.

[17] Z. Addadi, B. Doumi, A. Mokaddem, M. Elkeurti, A. Sayede, A. Tadjer et al., *Electronic and ferromagnetic properties of 3d (V)-doped (BaS) barium sulfide*, J. Supercond. Nov. Magn. **30** (2017) 917.

[18] M. Sajjad, S. Alay-e Abbas, H. Zhang, N. Noor, Y. Saeed, I. Shakir et al., *First principles study of structural, elastic, electronic and magnetic properties of Mn-doped AlY (Y= N, P, As) compounds*, J. Magn. Magn. Mater. **390** (2015) 78.

[19] M. M. Obeid, H. R. Jappor, S. J. Edrees, M. M. Shukur, R. Khenata and Y. Mogulkoc, *The electronic, half-metallic, and magnetic properties of $Ca_{1-x}Cr_xS$ ternary alloys: insights from the first-principle calculations*, J. Mol. Graph. Model. **89** (2019) 22.

[20] X. Zhang, Z. Quan, J. Yang, P. Yang, H. Lian and J. Lin, *Solvothermal synthesis of well-dispersed MF_2 (M= Ca, Sr, Ba) nanocrystals and their optical properties*, Nanotechnology **19** (2008) 075603.

[21] Z. Quan, D. Yang, C. Li, P. Yang, Z. Cheng, J. Yang et al., *SrF_2 hierarchical flowerlike structures: Solvothermal synthesis, formation mechanism, and optical properties*, Mater. Res. Bull. **44** (2009) 1009.

[22] Z. Wang, W. Han and H. Liu, *EDTA-assisted hydrothermal synthesis of cubic SrF_2 particles and their catalytic performance for the pyrolysis of 1-chloro-1, 1-difluoroethane to vinylidene fluoride*, CrystEngComm **21** (2019) 1691.

[23] G. W. Rubloff, *Far-ultraviolet reflectance spectra and the electronic structure of ionic crystals*, Phys. Rev. B **5** (1972) 662.

[24] I. Richman, *Longitudinal optical phonons in CaF_2, SrF_2, and BaF_2*, J. Chem. Phys. **41** (1964) 2836.

[25] S. Jiayue, X. Jianbo, X. Zhang and D. Haiyan, *Hydrothermal synthesis of $SrF_2:Yb^{3+}/Er^{3+}$ micro-/nanocrystals with multiform morphologies and upconversion properties*, J. Rare Earths. **29** (2011) 32.

[26] C. Zhang, Z. Hou, R. Chai, Z. Cheng, Z. Xu, C. Li et al., *Mesoporous SrF_2 and $SrF_2:Ln^{3+}$ (Ln= Ce, Tb, Yb, Er) hierarchical microspheres: hydrothermal synthesis, growing mechanism, and luminescent properties*, J. Phys. Chem. C **114** (2010) 6928.

[27] C. Park and S. Park, *Effective up-conversion behaviors for $Er^{3+}–Yb^{3+}$-doped SrF_2 phosphors synthesized by flux-assist method*, J. Mater. Sci.: Mater. Electron. **31** (2020) 832.

[28] W. Kohn and L. J. Sham, *Self-consistent equations including exchange and correlation effects*, Phys. Rev. **140** (1965) A1133.

[29] K. Schwarz and P. Blaha, *Solid state calculations using WIEN2k*, Comput. Mater. Sci. **28** (2003) 259.

[30] J. P. Perdew, A. Ruzsinszky, G. I. Csonka, O. A. Vydrov, G. E. Scuseria, L. A. Constantin et al., *Restoring the density-gradient expansion for exchange in solids and surfaces*, Phys. Rev. Lett. **100** (2008) 136406.

[31] A. Becke and E. Johnson, *A simple effective potential for exchange.*, J. Chem. Phys. **124** (2006) 221101.

[32] F. Tran, P. Blaha and K. Schwarz, *Band gap calculations with Becke–Johnson exchange potential*, J. Phys. Condens. Matter. **19** (2007) 196208.

[33] F. Tran and P. Blaha, *Accurate band gaps of semiconductors and insulators with a semilocal exchange-correlation potential*, Phys. Rev. Lett. **102** (2009) 226401.

[34] D. Koller, F. Tran and P. Blaha, *Improving the modified Becke-Johnson exchange potential*, Phys. Rev. B **85** (2012) 155109.

[35] H. J. Monkhorst and J. D. Pack, *Special points for brillouin-zone integrations*, Phys. Rev. B **13** (1976) 5188.

[36] F. Birch, *Finite strain isotherm and velocities for single-crystal and polycrystalline NaCl at high pressures and 300 K*, J. Geophys. Res. Solid Earth **83** (1978) 1257.

[37] R. Wyckoff, *Crystal Structures*, no. v. 1 in Crystal Structures. Wiley, 1963.

[38] L. Vegard, *Formation of mixed crystals by solid-state contact*, J. Phys. **5** (1921) 393.

[39] B. Jobst, D. Hommel, U. Lunz, T. Gerhard and G. Landwehr, *E 0 band-gap energy and lattice constant of ternary $Zn_{1-x}Mg_xSe$ as functions of composition*, Appl. Phys. Lett. **69** (1996) 97.

[40] F. E. H. Hassan and H. Akbarzadeh, *First-principles investigation of BN_xP_{1-x}, BN_xAs_{1-x} and BP_xAs_{1-x} ternary alloys*, Mater Sci Eng B Solid State Mater Adv Technol. **121** (2005) 170.

[41] S. Gehrsitz, H. Sigg, N. Herres, K. Bachem, K. Köhler and F. Reinhart, *Compositional dependence of the elastic constants and the lattice parameter of $Al_xGa_{1-x}As$*, Phys. Rev. B **60** (1999) 11601.

[42] G.-X. Miao and J. S. Moodera, *Spin manipulation with magnetic semiconductor barriers*, *Physical Chemistry Chemical Physics* **17** (2015) 751.

[43] J. Radovanović, V. Milanović, Z. Ikonić and D. Indjin, *Optimization of spin-filtering properties in diluted magnetic semiconductor heterostructures*, *Journal of applied physics* **99** (2006) 073905.

[44] S. Belbachir, C. Abbes, M. Belkaid and A. H. Belbachir, *First-principle study of structural, elastic, electronic and magnetic properties of the quaternary heusler CoZrFeP*, *J. Supercond. Nov. Magn.* **33** (2020) 2899.

[45] X. Li, J. Lu, G. Peng, L. Jin and S. Wei, *Solvothermal synthesis of MnF$_2$ nanocrystals and the first-principle study of its electronic structure*, *Journal of Physics and Chemistry of Solids* **70** (2009) 609.

[46] J. Zhao, H. Zhang, C. Niu, J. Zhang, Z. Zeng and X. Wang, *Investigations of high-pressure properties of mnf2 based on the first-principles method*, *The Journal of Physical Chemistry C* **125** (2021) 21709.